

CLEAR SKY DIURNAL BEHAVIOR OF TROPOSPHERIC SCINTILLATION AT KU-BAND SATELLITE COMMUNICATION IN EQUATORIAL MALAYSIA

Ibtihal F.El-Shami^a, Hong Yin Lam^b, Jafri Din^{a*}, Siat Ling Jong^c

^aDepartment of Communication Engineering, Faculty of Electrical Engineering, 81310 UTM Johor Bahru, Johor, Malaysia

^bDepartment of Electrical Engineering Technology, Faculty of Engineering Technology, UTHM, 86400 Batu Pahat, Johor, Malaysia.

^cDepartment of Communication Engineering, Faculty of Electrical and Electronic Engineering, UTHM, 86400 Batu Pahat, Johor, Malaysia.

Article history

Received

31 March 2015

Received in revised form

30 June 2015

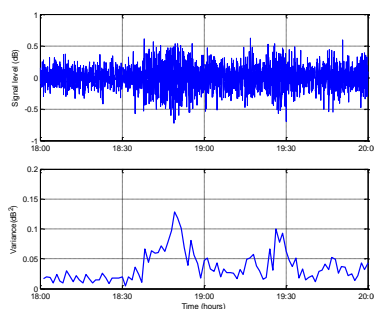
Accepted

20 August 2015

*Corresponding author

jafri@utm.my

Graphical abstract



Abstract

Tropospheric scintillation is referred to rapid fluctuation of received signal amplitude. It can cause propagation impairments that affect satellite communication systems operating at above 10 GHz of frequency. In this work, we have exploited 1 year of measured broadcasting signal data collected in Johor, Malaysia to investigate the effects of scintillation intensity on a SatCom system operating at 11.075 GHz with its links pointed towards the MEASAT-1 satellite (an elevation angle of 75.61°). We have investigated the behavior of this scintillation amplitude through the classification and analysis of a time-series satellite broadcasting signal and have then compared the statistical results with existing scintillation prediction models. The comparison results indicate that there is a significant discrepancy between measured data and those models and that the performance of these prediction models does not appear to be satisfactory, with the exception of the ITU-R and the Ortgies Refractivity model. In addition, we have investigated the diurnal behavior of the scintillation intensity at four different periods of the day and proposed a modified Marzano model to accommodate local meteorological input parameters. The models performances are assessed against the available measurement dataset. The proposed models provide system operators and radio communication engineers with critical information on the fluctuations of tropospheric scintillation variance on the satellite signal during a typical day taken into the account of local meteorological peculiarities.

Keywords: Diurnal Variations, equatorial region, radiowave propagation, satellite communications, Tropospheric scintillation

Abstrak

Ayunan pantas amplitud isyarat penerima yang lebih dikenali sebagai sintilasi troposfera merupakan salah satu faktor penting yang akan menghasilkan rosotan perambatan yang mempengaruhi sistem komunikasi satelit beroperasi pada frekuensi melebihi 10 GHz. Dalam penyelidikan ini, isyarat penyiaran di Johor yang dikumpul selama setahun telah dieksploitasi untuk kajian kesan keamatan sintilasi pada sistem satelit yang beroperasi pada frekuensi 11.075 GHz satelit MEASAT-1 (sudut dongakan 75.61 °). Kelakuan amplitud sintilasi itu diasas melalui klasifikasi dan analisis isyarat masa penyiaran siri satelit dan seterusnya keputusan statistik mereka dibandingkan dengan model ramalan sintilasi. Hasil perbandingan menunjukkan perbezaan yang ketara diantara prestasi model ramalan dengan data sintilasi kecuali model ITU-R dan Ortgies N. Selain daripada itu, ciri-ciri diurnal

intensiti sintilasi juga disiasat dalam empat masa yang berbeza dalam sehari dan satu model terubah Marzano telah dicadangkan untuk mengambilkira parameter meteorologi tempatan. Prestasi model ini telah dinilai dengan perbandingan data set sediaada. Model yang dicadangkan ini menyalurkan informasi kritikal mengenai ayunan amplitud isyarat satelit pada selang masa sepanjang hari untuk operator sistem serta jurutera radio komunikasi.

© 2015 Penerbit UTM Press. All rights reserved

1.0 INTRODUCTION

Satellite communication systems operating at low fade margins with a frequency above 10 GHz are exposed to the turbulent fluctuations of the refractive index, which cause random fading and enhancement of the received signal. This propagation mechanism, which affects the received signal level, is known as tropospheric scintillation. The rapid fluctuation of the received signal amplitude can range up to several decibels. The intensity of the fluctuations in the refractive index can produce significant impairments as the margin of the communications systems decreases. It is therefore of key importance to investigate the characteristics of this phenomena for the optimization of channel capacity [1]. To date, numerous experimental measurements have been carried out in several locations [1]–[3], and various models have been proposed for predicting the amplitude fluctuations [2]–[4]. However, only a few slant-path tropospheric scintillation results in the Malaysian equatorial region have been published, such as the study presented in [5]. The experimental results from these studies serve as a critical resource for evaluating the performance of various prediction models that are available for this region.

Generally, the fluctuation of the electromagnetic wave signal passing through the atmospheric medium is primarily due to turbulent irregularities in temperature, humidity and pressure [6]. The impact of the behaviour or features of those parameters on scintillation is of key importance, particularly in the equatorial region which is often dominated by local climatic peculiarities (e.g. diurnal variation [7]). Various studies have been carried out to predict the clear-sky tropospheric scintillation, using in particular, diurnal behaviour related to the hour of the day. Unfortunately, most of the models developed are based on the measurement database in temperate regions [8]–[9]. Similar studies that focus on this aspect in heavy rain regions are still very rare, with the exception of [5]. Hence, it is worthwhile to further investigate the diurnal variations of scintillation in this heavy rain region, as well as their relationship to meteorological parameters, such as temperature, humidity and atmospheric refractive index.

In this work, we have investigated the clear-sky scintillation effects in equatorial Johor by exploiting a year of scintillation measurements from a commercial broadcasting satellite link at 11.075 GHz in equatorial

Malaysia. The rest of this paper is organized as follows. First, the main features of the five currently accepted prediction models [2]–[4],[10] are briefly explained in Section 2. This is followed by a description of the measurement setup, as well as the data processing performed, in Section 3. The dynamic behaviour of clear-sky scintillations and relationship with meteorological parameters are presented in Section 4. Section 5 introduces a local diurnal variations model for the prediction of scintillations amplitude variance, as well as the performance evaluations of this model against the satellite measurement data. Finally, Section 6 summarizes and draws some conclusions.

2.0 SCINTILLATION PREDICTION MODELS

Several prediction models have been developed and proposed for the evaluation of clear sky statistical distributions of scintillation [2]–[4], [10]. Most of these prediction models are based on both theoretical studies and experimental results. In addition, most of the models require various inputs related to link parameters, such as frequency, elevation angle and antenna diameter [10]. Furthermore, local meteorological data (i.e. humidity at ground level and mean temperature) are also essential for the reliable prediction of scintillation amplitude [2], [4],[10].

2.1 Karasawa Scintillation Model

The Karasawa prediction model [2] is the most well-known model for the prediction of clear-sky scintillation amplitudes. This model was developed based on data collected from the INTELSAT-V satellite (with the beacon receiver horizontally polarized at Yamaguchi, Japan at a low elevation angle of 6.5° and operating at a frequency of 14/11 GHz). The Cassegrain antenna used has a diameter of 7.6 m and a data sampling interval of 1 second. In this model, long-term scintillation variance is expressed in relation to the wet term reflectivity N_{wet} [2]:

$$\sigma_x = \sigma_{x,ref} \cdot \eta_f \cdot \eta_\theta \cdot \eta_D \quad (1)$$

where:

$$\sigma_{x,ref} = 0.15 + 5.2 \times 10^{-3} N_{wet} \quad (2)$$

$$\eta_f = (f / 11.5)^{0.45} \quad (3)$$

$$\eta_\theta = \left(\sin 6.5^\circ / \sin \theta \right)^{1.3} \quad \theta \geq 5^\circ \quad (4)$$

$$\eta_D = \sqrt{\frac{G(D)}{G(7.6)}} \quad (5)$$

$$N_{wet} = \frac{3732 H e_s}{(273 + T)^2} \quad (6)$$

where t is the average temperature ($^\circ\text{C}$), H is the relative humidity (%), and e_s is the saturated vapour, which can be approximated by t , in the following equation:

$$e_s = 6.11 e^{\frac{19.7t}{t+273}} \quad (\text{mb}) \quad (7)$$

The antenna aperture averaging factor G is given by:

$$G(R) = \begin{cases} 1 - 1.4 \left(\frac{R}{\sqrt{\lambda L}} \right), & \text{for } 0 \leq \frac{R}{\sqrt{\lambda L}} \leq 0.5 \\ 0.5 - 0.4 \left(\frac{R}{\sqrt{\lambda L}} \right), & \text{for } 0.5 \leq \frac{R}{\sqrt{\lambda L}} \leq 1 \\ 0.1, & \text{for } 1 < \frac{R}{\sqrt{\lambda L}} \end{cases} \quad (8)$$

where

R effective radius of circular antenna aperture (m), given by:

$$R = 0.75 \left[\frac{D_a}{2} \right] \quad (9)$$

D_a physical diameter of reflector (m),

λ operating wavelength (m),

L slant distance to height of a horizontal thin turbulent layer given by

$$L = \frac{2h}{\sqrt{\sin^2 \theta + 2.35 \times 10^{-4} + \sin \theta}} \quad (10)$$

Finally, signal level variation $X(p)$ expressed as a function of time percentage p in terms of cumulative distribution is given by

$$X(p) = \eta(p) \times \sigma_x(f, \theta, D_a, t, H) \quad (11)$$

where time percentage factor enhancement η and fade are given by either (12) or (13):

$$\eta(p) = -0.0597 \times (\log \log p)^3 - 0.0835 \times (\log \log p)^2 - 1.258 \times (\log \log p) + 2.672 \quad (\text{signal enhancement}) \quad (12)$$

$$\eta(p) = -0.061 \times (\log \log p)^3 + 0.072 \times (\log \log p)^2 - 1.71 \times (\log \log p) + 3, \quad \text{for } 0.01 \leq p \leq 50 \quad (\text{signal fading}) \quad (13)$$

2.2 ITU-R Scintillation Prediction Model

The International Telecommunication Union - Radio communication Sector (ITU-R) model was developed primarily based on the Karasawa model. It provides a general technique for predicting the cumulative

distribution of tropospheric scintillation with frequencies between 7 and 20 GHz. The ITU-R model [4] is based on monthly temperature t ($^\circ\text{C}$) and relative humidity H as well as signal frequency f (GHz), antenna diameter D_a (m) and path elevation angle θ (ITU-R P.618-10, 2009 [4]).

The standard deviation of the signal σ for the considered period and propagation path can be obtained by [4]:

$$\sigma = \sigma_{ref} f^{7/12} \frac{g(x)}{(\sin \theta)^{1.2}} \quad (14)$$

where:

$$\sigma_{ref} = 3.6 \times 10^{-3} + N_{wet} \times 10^{-4} \quad [\text{dB}] \quad (15)$$

The ITU-R antenna aperture averaging factor $g(x)$ is given by:

$$g(x) = \sqrt{3.86 (x^2 + 1)^{11/12} \cdot \sin \left[\frac{11}{6} \arctan \frac{1}{x} \right] - 7.08 x^{56}} \quad (16)$$

$$\text{with } x = 1.22 D_{eff}^2 (f / L) \quad (17)$$

$$\text{where } D_{eff} = \sqrt{\eta} D \quad [\text{m}] \quad (18)$$

2.3 Otung Scintillation Prediction Model

The Otung scintillation model [3] is a modified ITU-R scintillation model developed based on the data obtained at Sparsholt, UK (51.5850' N, 1.5033' W) over a one-year period using the Olympus satellite 19.7704 GHz beacon viewed at a nominal elevation of 28.74°. The scintillation data are collected using a 1.2 m diameter beacon with a 10 Hz sampling rate. Raw data were pre-processed through a high-pass filter with a cut-off frequency of 0.004 Hz to avoid attenuation of the signal, which could lead to inaccurate processing. The average scintillation intensity σ_{pre} can be predicted as

$$\sigma_{pre} = \frac{\sigma_{ref} f^{7/12} g(x)}{(\sin \theta)^{11/12}} \quad (19)$$

The scintillation fade χ_{-a} (dB), scintillation enhancement χ_{+a} (dB) and scintillation intensity σ_x (dB) are given by:

$$\chi_{+a} = 3.1782 \sigma_{pre} \exp \left[\frac{-0.35965 p}{-(0.272113 - 0.00438 p) \ln(p)} \right] \quad (20)$$

$$\chi_{-a} = 3.6191 \sigma_{pre} \exp \left[\frac{-9.50142 * 10^{-4}}{p} \right] \left[\frac{-0.40454 - 0.00285 p}{\ln(p)} \right] \quad (21)$$

$$\sigma_{\chi} = 2.847\sigma_{pre} \exp \left[\frac{0.01827p - \{0.345529 + 5.00745 \times 10^{-3} p\} \ln(p)}{p} \right] \quad (22)$$

2.4 Ortgies Prediction Models

The Ortgies models [10] generally consist of two different models, Ortgies-Refractivity (Ortgies-N) and Ortgies-Temperature (Ortgies-T). These two models are based on the direct linear relationships between mean surface measurement and monthly mean normalized log variance of scintillation $\ln(\sigma_x^2)$ [10]. The experimental data were taken from Olympus satellite measurements at Darmstadt, Germany. The frequencies used for these models were 12.5, 20 and 30 GHz. Both models introduce a log-normal probability density function (pdf) for the prediction of the long-term distribution of scintillation intensity. The parameters μ and s are the mean and standard deviation of $\ln(\sigma_x^2)$, respectively. The Ortgies-T model requires the monthly mean surface temperature (T) as an input to the model below:

$$\ln \sigma_{pre}^2 = \ln \left(g(x) \cdot f^{1.21} (\sin \theta)^{-2.4} \right) - 1.25 + 0.0865T \quad (23)$$

while the Ortgies-N model considers the monthly mean log-variance of signal log amplitude to monthly mean wet component of surface refractivity (N_{wet}) as an input parameter:

$$\ln \sigma_{pre}^2 = \ln \left(g(x) \cdot f^{1.21} (\sin \theta)^{-2.4} \right) - 13.45 + 0.0462N_{wet} \quad (24)$$

3.0 EXPERIMENTAL SETUP AND DATA PROCESSING

The experimental station installed in the premises of Universiti Teknologi Malaysia consists of one direct broadcast receiving antenna with a diameter of 60 cm pointed towards Malaysia East Asia Satellite-1 (MEASAT-1), a broadcasting satellite at an elevation angle of 75.61°. The broadcasting signal at 11.075 GHz is monitored and recorded using a spectrum analyzer and data logger. An automatic weather station is also located at a meteorological station, which is equipped with various sensors and a tipping bucket rain gauge. The meteorological station is placed near the receiver antenna. The experimental setup is illustrated in Figure 1 and the details of experimental setup can be found in [11].

One year of experimental data from March 2001 to February 2002 were processed and separated into clear-sky and rainy events based on data from a rain gauge located near the receiving antenna. The scintillation contribution was carefully extracted from the time series of the signal level (1 sample/sec) using a fifth-order Butterworth high-pass filter with a cut-off frequency of 0.025 Hz [12].

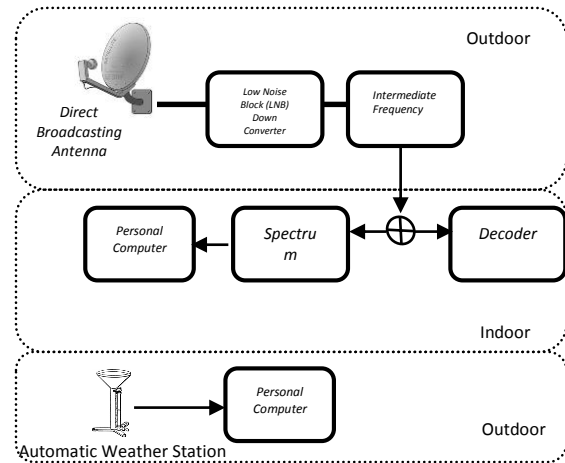


Figure 1 Block diagram of experimental setup

After the filtering process, the cumulative probability density function of scintillation intensity for all clear sky periods was determined. This was compared with the five models presented above to assess their performance in and applicability to the particular Malaysian equatorial region. In addition, the diurnal behaviours of the scintillation intensity were investigated within four non-overlapping time of day intervals: 00:00-06:00, 06:00-12:00, 12:00-18:00 and 18:00-24:00.

4.0 THE DIURNAL BEHAVIOR OF CLEAR-SKY SCINTILLATION AND METEOROLOGICAL EVIDENCES

Figure 2 shows typical recordings of tropospheric scintillation at 11.075 GHz, as well as the variance extracted. The signal levels fluctuated about 1.2 dB peak-to-peak with a maximum variance of approximately $\sim 0.13 dB^2$.

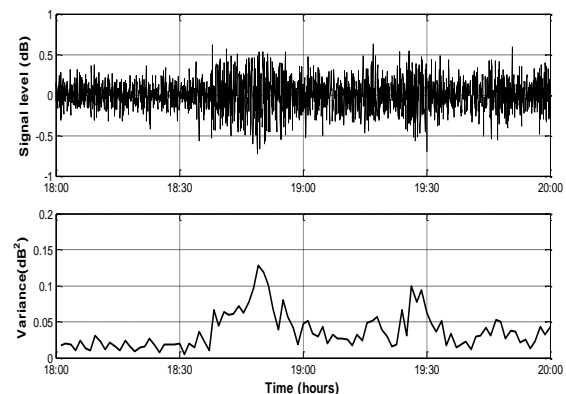


Figure 2 Typical example of tropospheric scintillation and its variance.

Figure 3(a) shows a three-dimensional plot of mean scintillation variance as a function of the mean surface temperature and month index. It seems to

give an indication that the scintillation effect occurs primarily in the evening hours.

Similar three-dimensional plots of surface temperature, relative humidity and wet refractivity (N_{wet}) are also shown in Figure 3(b)-(d). The plots confirm that different time of day intervals have different temperatures and humidity levels. However, the monthly mean values of temperature and relative humidity were approximately the same throughout the year. This finding confirms a positive correlation between scintillation intensity and ground temperature and a negative correlation between scintillation intensity and ground relative humidity.

Beside the meteorological characteristics of different time periods, a preliminary comparison activity was also made of the measured scintillation fade and enhancement with all the prediction models. This comparison is shown in Figure 4. At first glance, almost all the prediction models seem to underestimate the measured scintillation in this area. However, The ITU-R and Ortgies-N models appear to most closely fit to the measured results. The other models clearly underestimated the measurements.

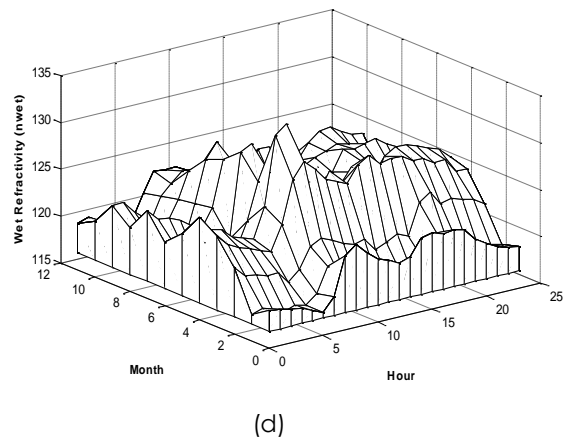
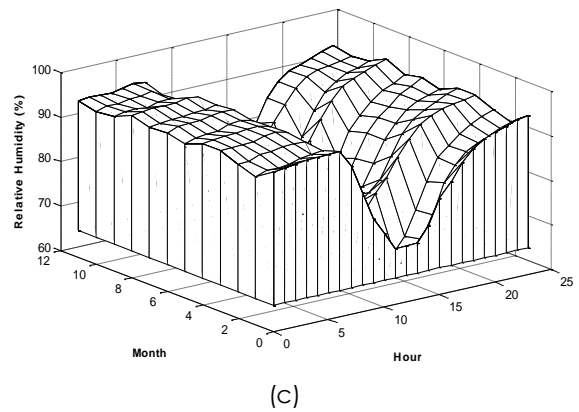
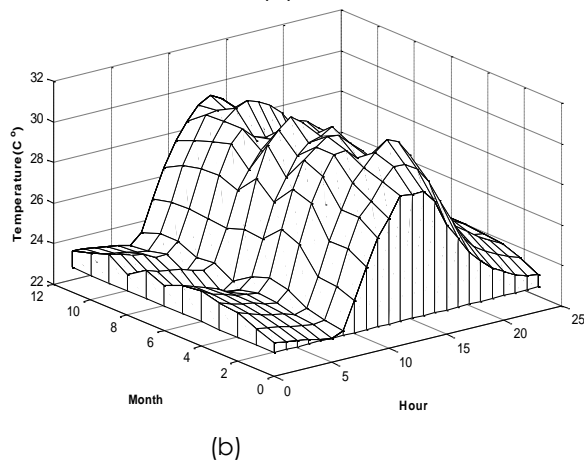
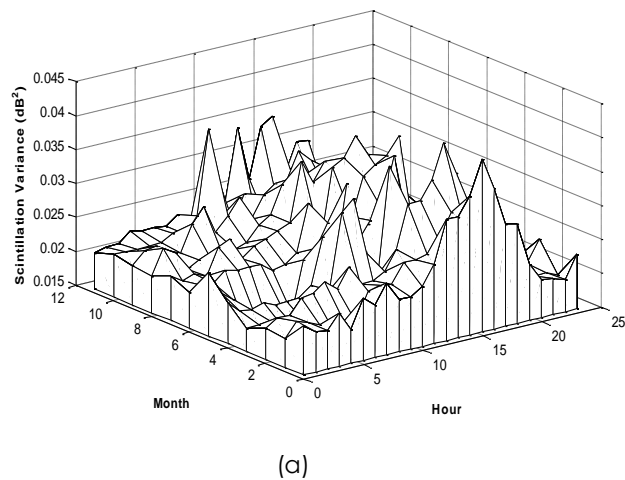


Figure 3 Diurnal and seasonal variation of 11.075 GHz MEASAT scintillation variance (a), ground temperature (b), ground relative humidity (c) and ground wet refractivity index N_{wet} (d) for 2001 as measured at Skudai, Johor.

These findings are in agreement with the findings of Mandeep *et al.* [5], who also found the ITU-R model to be the closest match to their experimental results. There is no evidence that turbulence induced refractive irregularities in the tropics are different than those noted elsewhere. However, Touw and Herben [13] pointed out that the vertical extent over which the turbulent irregularities can exist might be larger, which could enhance the average scintillation intensity.

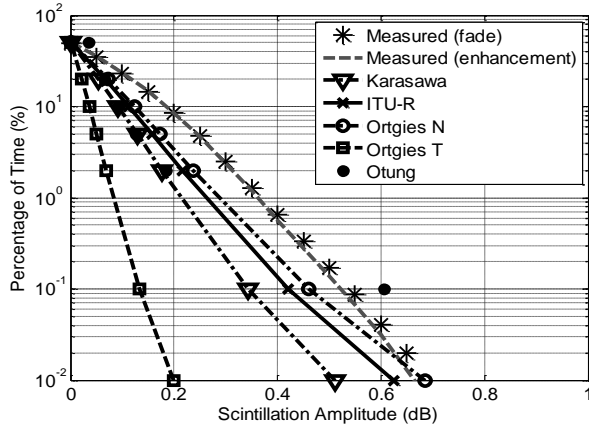


Figure 4 Complementary Cumulative Distribution Function (CCDF) of the measured scintillation fade and enhancement in equatorial Johor compared with the various statistical scintillation prediction models.

Based on the evidence of scintillation varying throughout different times of day, we extended our analysis to the diurnal behaviour of scintillation intensity divided into four time intervals, as mentioned in Section 3 above.

Figure 5 shows the diurnal behaviour of scintillation intensity from the measured satellite signal during different time intervals of the day. The results clearly show that higher scintillation intensities are more likely to occur during the morning and afternoon periods. Such findings will provide critical information for communication system operators and system designers in the Malaysian equatorial region, as the fluctuation intensity of the refractive-index may vary depending on local climatic conditions. For this reason, the next section will focus on the development of a diurnal amplitude scintillation variance model that employs local meteorological inputs, such as temperature and relative humidity.

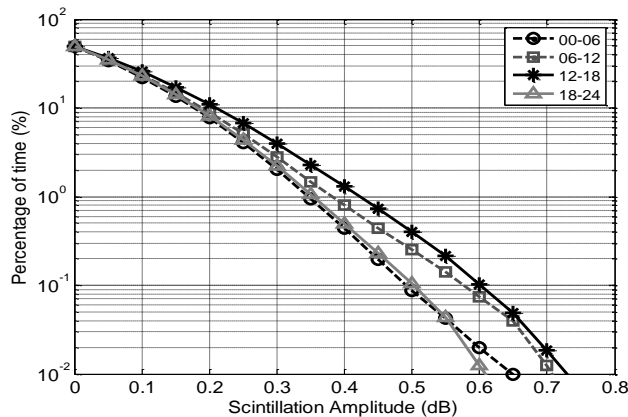


Figure 5 Measured diurnal behaviour of the scintillation intensity extracted from the MEASAT-1 broadcasting satellite signal.

5.0 DIURNAL MODEL OF EQUATORIAL TROPOSPHERIC SCINTILLATION

5.1 Relationships of Diurnal Scintillation Variance and Surface Meteorological Data

As mentioned previously, scintillation variance throughout the day is characterized by surface meteorological parameters. The temperature and relative humidity, in particular, play an important role in predicting the diurnal behaviour of scintillation variance.

For this reason, statistical multivariate regression was employed to develop several prediction models of amplitude scintillation variance with respect to the combination of surface temperature and relative humidity. Normalized mean scintillation variance $\langle \sigma^2 x \rangle_n$ as introduced in [14] will be used as follows:

$$\langle \sigma_x^2 \rangle_n = \frac{\langle \sigma_x^2 \rangle}{G^2 f^\alpha (\sin \theta)^{-\beta}} \tag{25}$$

where α and β are the frequency scaling exponent and the elevation scaling exponent, respectively. G is the antenna averaging factor as suggested in [2].

From the perspective of long-term statistics, the probability density function (pdf) of $\langle \sigma^2 x \rangle$ can be modelled by a log-normal pdf as :

$$p(\langle \sigma^2 \rangle) = \frac{1}{\sqrt{2\pi s_\sigma^2} \langle \sigma_x^2 \rangle} \exp \left[-\frac{(\ln \langle \sigma_x^2 \rangle - m_\sigma)^2}{2s_\sigma^2} \right] \tag{26}$$

where m_σ and s_σ are the mean and the standard deviation of the scintillation log-variance $\ln(\langle \sigma^2 x \rangle)$, respectively. Hence the normalization of mean scintillation log-variance can be expressed by:

$$m_{\sigma_n} = \overline{\ln \langle \sigma_x^2 \rangle_n} = m_\sigma + \ln \left(\frac{1}{G^2 f^\alpha (\sin \theta)^{-\beta}} \right) \tag{27}$$

where the over bar represents the long-term temporal average.

The relationships of diurnal scintillation variance and surface meteorological parameters are inferred from the variation of the signal strength measured by the 11.075 GHz MEASAT-1 satellite in 2001 and meteorological ground-based measurements in Universiti Teknologi Malaysia (UTM).

Figure 6 shows the normalized log-variance $\ln \langle \sigma_x^2 \rangle_n$ on an hourly basis as a function of the surface temperature T_s (a) and the surface relative humidity RH_s (b) obtained from the one year data set.

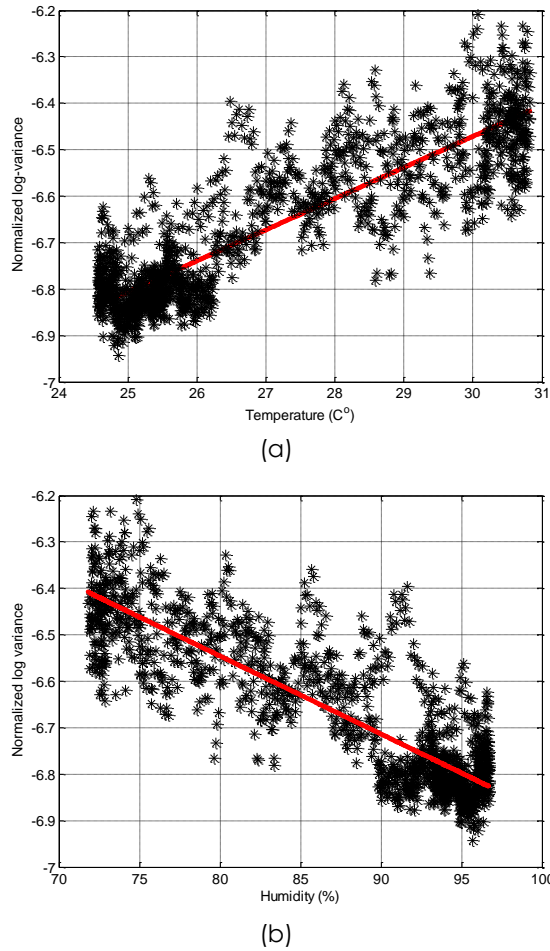


Figure 6 Normalized scintillation log-variance ($\ln(\sigma_x^2)_n$) on an hourly basis as a function of surface temperature (a) and surface relative humidity (b), derived from the one year data set.

As can be clearly observed, the linear relationship of temperature and relative humidity with $\ln(\sigma_x^2)_n$ can be ascribed to the strong influence of temperature on scintillation, and indirectly to relative humidity and wind velocity [15]. Solar heating of the ground increases the surface air temperature, resulting in a layer of warm air at the surface and producing instability and scintillation. On the other hand, there is generally a decrease in relative humidity due to warmer air holding more moisture, thus increasing the saturated water-vapour pressure [16].

It is also worth noting that the linear relationship between $\ln(\sigma_x^2)_n$ and T_s can be represented by:

$$\ln \sigma_{xn}^2 = -8.464 + 0.06644T_s \quad (28)$$

while $\ln(\sigma_x^2)_n$ and RH_s can be represented by a quadratic best fitting as follows:

$$\ln \sigma_{xn}^2 = -6.538 + 0.01485RH_s - 0.0001853RH_s^2 \quad (29)$$

The correlation between $\ln(\sigma_x^2)_n$ and T_s is 0.75 on an hourly basis, while the correlation between $\ln(\sigma_x^2)_n$ and RH_s is 0.73.

In addition to temperature and relative humidity, the atmospheric refractive index is another meteorological parameter that influences signal fluctuations. Surface-wet refractivity N_{wet} which is a function of water vapour pressure and temperature should be taken into account when developing the diurnal scintillation variation model. Figure 7 illustrates the relationship between $\ln(\sigma_x^2)_n$ and N_{wet} on an hourly basis, with a correlation of 0.43. This parameter can be fitted with the following the quadratic model:

$$\ln \sigma_{xn}^2 = -206.4 + 3.008N_{wet} - 0.01132N_{wet}^2 \quad (30)$$

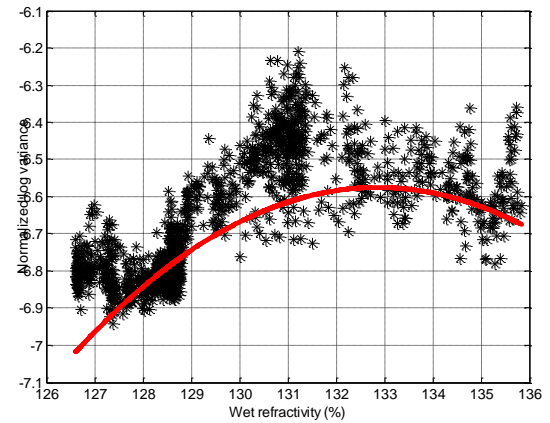


Figure 7 Normalized scintillation log-variance ($\ln(\sigma_x^2)_n$) on an hourly basis as a function of surface wet refractivity.

5.2 Prediction of Scintillation Parameters

The prediction of signal fluctuation as a function of diurnal variation is closely related to the meteorological process. This process depends on variations of temperature; T_s , relative humidity; RH_s and surface atmospheric wet refractive index N_{wet} . To estimate the best $\ln(\sigma_x^2)_n$ on an hourly basis, various combination of these three parameters have been evaluated through a best fit procedure by considering different types of analytical curves. Linear and quadratic fits were determined to be the most accurate and suitable for these estimations. The estimation results are shown in Table 1, in which root mean square (RMS) errors and correlation coefficients for the 10 combination models are compared.

Testing has confirmed that quadratic estimators using mix meteorological data would perform better than a linear relationship estimator. Obviously, the best estimators are quadratic fits of the T_s - RH_s and T_s - N_{wet} models. This finding is similar to the one proposed for temperate regions [14].

Table 1 Results of the statistical regression comparison to estimate the normalized log variances on an hourly basis

Predictors	RMS	correlation
T_s (linear)	0.081	0.7533
RH_s (linear)	0.0837	0.7369
N_{wet} (linear)	0.1222	0.4385
$T_s - RH_s$ (linear)	0.0807	0.7552
$T_s - N_{wet}$ (linear)	0.0806	0.7558
T_s (quadratic)	0.0802	0.7584
RH_s (quadratic)	0.0832	0.7399
N_{wet} (quadratic)	0.1023	0.607
$T_s - RH_s$ (quadratic)	0.0704	0.8143
$T_s - N_{wet}$ (quadratic)	0.0754	0.7867

Both Predictors contain the following expression on an hourly basis:

$$\langle \sigma_x^2 \rangle_n = \exp(a_0 + a_1 T_s + a_2 RH_s + a_3 T_s^2 + a_4 T_s RH_s + a_5 RH_s^2) \quad (31)$$

$$\langle \sigma_x^2 \rangle_n = \exp(b_0 + b_1 T_s + b_2 N_{wet} + b_3 T_s^2 + b_4 T_s N_{wet} + b_5 N_{wet}^2) \quad (32)$$

Table 2 lists the resulting regression coefficients for (31) and (32), based on one year of hourly data.

Table 2 Regression coefficients of (31) and (32)

Hourly Basis	Equation (31)	Equation (32)
a_0	995.6	36.24
a_1	-38.55	2.115
a_2	-11	-1.107
a_3	0.3702	0.00598
a_4	0.2121	-0.0018
a_5	0.03006	0.006129

To assess the effectiveness of the above estimation methods, we compared the prediction of scintillation variance on an hourly basis to the measured scintillation extracted from the 11 GHz MEASAT broadcasting satellite as shown in Figure 8. The performance of the estimator from (27) and (28) can be quantified by calculating RMS error values on an hourly basis. Figure 9 shows the assessment of these models together with the original models [14], STH2 (based on surface temperature and humidity in quadratic form) and STN2 (based on surface temperature and wet refractivity in quadratic form). This result clearly indicates the importance of using local input meteorological data to obtain good estimates of scintillation variances.

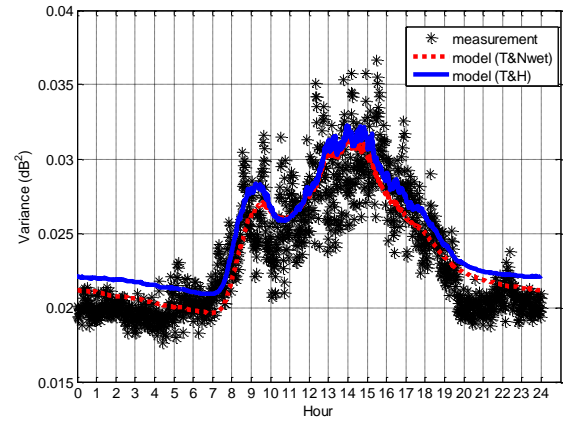


Figure 8 MEASAT measured scintillation variance at 11.075 GHz and 75.61° elevation angle compare with the estimated variance on an hourly basis.

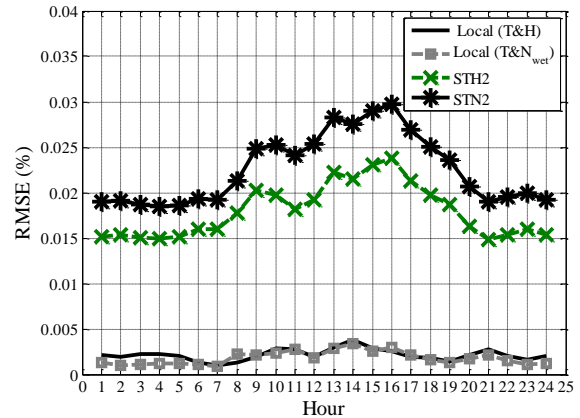


Figure 9 Root mean square value of the error for prediction of diurnal variations scintillation variance. Comparison between local models and Marzano model [14].

6.0 CONCLUSION

This research investigated diurnal variations of tropospheric scintillation in equatorial Johor, Malaysia (a Heavy rain region) and proposed a modified Marzano model [14] that takes advantage of local meteorological parameter such as temperature, humidity and atmospheric refractive index. Two local diurnal models are proposed. One model combined temperature and humidity. The other model combined temperature and wet refractive index. These models are found to be in good agreement with the hourly measurements from MEASAT-1 broadcasting satellite. Such models provide crucial information for system designers and service providers regarding the critical time periods that should receive particular attention when seeking to provide low fade margin systems.

Acknowledgement

This work has been funded by Ministry of Education Malaysia and UTM under "Research University Grant" Vot. No. Q.J.130000.2523.07H50 and "FRGS" Vot. No. R.J.130000.7823.4F320.

References

- [1] G. P. Pedro, J. M. Riera, and A. Benarroch. 2012. "Tropospheric Scintillation With Concurrent Rain Attenuation at 50 GHz in Madrid," *IEEE Trans. Antennas Propag.* 60 (3) : 1578–1583.
- [2] Karasawa, Yoshio, Matsuichi Yamada, and Jeremy E. Allnutt. 1988. "A New Prediction Method for Tropospheric Scintillation on Earth-Space Paths," *IEEE Transactions on Antennas and Propagation.* 36 (11): 1608-1614.
- [3] Otung, I.E., 1996. "Prediction Of Tropospheric Amplitude Scintillation On A Satellite Link" *IEEE Transactions on Antennas and Propagation.* 44(12): 1600-1608.
- [4] Propagation Data And Prediction Methods Required For The Design Of Earth-Space Telecommunication Systems". Recommendation ITU-R.P 618-10. 2009.
- [5] A. C. C. Y. J.S. Mandeep, M. Abdullah and M.Tariqul. 2011."Comparison and Analysis of Tropospheric Scintillation Models for Northern Malaysia," *Acta Astronautica.* 69 :2-5.
- [6] M.J.L. van de Kamp, C. Riva, J.K. Trevenen, and E.T. Solonen. 1999. "Frequency Dependence Of Amplitude Scintillation" *IEEE Transactions on Antennas and Propagation.* 47(1): 77-85.
- [7] H.Y. Lam, L. Luini, J. Din, C. Capsoni, A. D. Panagopoulos. "Investigation of Rain Attenuation in Equatorial Kuala Lumpur". *IEEE Antennas and Wireless Propagation Letters.* 11 : 1002-1005.
- [8] A. Vander Vorst, D. Vanhoenacker, and L. Mercier. 1982. "Fluctuations On OTS-Earth Copolar Link Against Diurnal And Seasonal Variations," *Electron.Lett.* 18 : 915–917.
- [9] I. E. Otung, M. S. Mahmoud, and J. R. Norbury. 1995. "Radiowave Amplitude Scintillation Intensity: Olympus Satellite Measurements And Empirical Model," *Electron. Lett.* 31 : 1873–1875.
- [10] Ortgies G. 1985. Probability Density Function of Amplitude Scintillations. *Electronics Letters.* 21 (4): 141-142.
- [11] Jong, S. L., D'Amico, M., Din, L. and Lam, H. Y. 2014. Analysis of Fade Dynamic at Ku-band in Malaysia. *International Journal of Antennas and Propagation:* 1-7.
- [12] G. P. Pedro, J. M. Riera, and A. Benarroch. 2007. "Measurements Of Tropospheric Scintillation On Millimetre-Wave Satellite Link," *IET Electronics Letters.* 43 (22).
- [13] S. I. E. Touw and M. H. A. J. Herben. 1996. "Short-Term Frequency Scaling Of Clear-Sky And Wet Amplitude Scintillation," *IEE Proc.-Microw. Antennas Propag.* 143(6): 521–526.
- [14] F. S. Marzano and G. d'Auria. 1998. "Model-Based Prediction of Amplitude Scintillation Variance Due to Clear-Air Tropospheric Turbulence on Earth-Satellite Microwave Links," *IEEE Transactions on Antennas and Propagation.* 46 (10).
- [15] O. P. Banjo and E. Vilar. 1987. "The Dependence Of Slant Path Amplitude Scintillations On Various Meteorological Parameters," in Proc. 5th Int. Conf. *Antennas Propagat.* (ICAP'87), York, U.K : 277–280.
- [16] U. Merlo, E. Fionda, and J. Wang. 1987. "Ground Level Refractivity And Scintillation In Space-Earth Links," *Appl. Opt.* 27: 2247–2252.